Static and free vibration analyses of a bike using finite element method

Chia-Chin Wu[1], Donald Ballance[2]

[1]Technology Department, SuperAlloy Industrial Co., Ltd., Yun-Lin, Taiwan
[2]Department of Mechanical Engineering, University of Glasgow, Glasgow, UK

Abstract— *A successfully designed bike should possess safety and comfort for the riders. A safe bike means that its structure must be strong enough to prevent from damage due to various external loads and a comfortable bike means that its suspension systems must be excellent enough to reduce the transmissibility of disturbance coming from the uneven roads to the rider. In order to achieve the above goals, various methods have been presented; however, most of them assumed that each part of a bike is a "rigid body" except the helical (coil) springs. For the last reason, this paper tries to use more versatile finite element method (FEM) to perform the static and free vibration analysis of a bike. It is believed that a finite element model with all parts of a bike replaced by the "elastic" elements or lumped masses should be more realistic. In this paper, the entire bike structure is modeled by using three kinds of beam elements: pinned-pinned (P-P), pinned-clamped (P-C) and clamped-clamped (C-C) beam elements. Among the main parts of a bike structure, the main frame and rim are modeled by the C-C elements, the elastic effect of each tire is modeled by using a P-C element, and each spoke or each "spring-damper unit" is modeled by a P-P element. The key point of this paper is to study the influence of some pertinent parameters on the lowest several natural frequencies and mode shapes of the bike. It is found that the radius of the hub (disks), the pretension of each spoke, the mass of various attachments or rider, and the riding gesture of a rider have significant influence on the free vibration characteristics, the static deformations and internal forces (and moments) of the pertinent structural members of a bike. Because the mass of a rider is much greater than that of the bike structure itself, the static and dynamic characteristics of a bike with and without a rider on it must be studied, separately.*

Keywords— Rider, Bike, Suspension System, Finite Element Method, Elastic Element, Lumped Mass, Main Frame, Rim, Tire, Spoke, Natural Frequency, Mode Shape

I. INTRODUCTION

In Ref. [1], Champoux et al. have indicated that "the more manufactures can learn and understand about the dynamic response of their products, the more they will be able to benefit both current and potential riders". It is the last reason, some researchers have devoted themselves to the study of vibration characteristics of bikes [1-4]. Besides, under the assumption that each part of the bike is a "rigid body" except the helical (coil) springs, some researchers paid their attentions to the design of rear suspension system of mountain bikes to improve the riding performance and rider comfort [4-8]. Since the conventional finite element method (FEM) with the entire bike structure replaced by a number of "elastic" members and lumped masses is more able to model a bike "accurately" and "realistically", and it can be used to study both the dynamic and static characteristics of bikes appearing in the foregoing literature [1-8], the objective of this paper is to continue the static and dynamic analyses of mountain bikes of Ref. [4] by using the FEM.

In general, an entire bike is composed of several sub-systems, such as the power transmission system, speed adjusting system, braking system, turning system, main frame and wheels. Among various parts of the entire bike, only those affecting its stiffness matrix are modeled by finite elements and those contributing to the overall mass matrix only are considered as the lumped masses attached to the associated nodes. Based on the last concept, the particulars for the finite element model of the bike studied in this paper are stated as follows: (i) The head tube, the front fork and the main frame (including top tube, down tube, seat post, seat stay and chain stay) are modeled by using the two-node clamped-clamped (C-C) beam elements [9], and a few of the last C-C beam elements are replaced by the pinned-clamped (P-C) ones [10] if one of two nodes of a C-C beam element is pinned. (ii) The front and rear rims are similar to the circular rings, thus, each on them are modeled by using a number of two-node C-C straight beam elements [11]; for convenience, the total number of beam elements for each rim is taken to be the same as that of the spokes on each rim. (iii) Since the stiffness of front or rear hub is much greater than the stiffness of each of the attaching spokes, thus, either front or rear hub is assumed to be a rigid body and each spoke

connecting a hub and the associated rim is modeled by a pinned-pinned (P-P) beam element. (iv) The total mass of each tire is uniformly distributed along the circumference of the associated rim and considered as part of the rim mass per unit length (i.e., the effective mass density of the rim is determined by $\overline{\rho}_r = \rho_{\text{rim}} + \overline{\rho}_{\text{tire}}$ with ρ_{rim} denoting the mass density of the rim material itself and $\overline{\rho}_{\text{tire}}$ denoting the equivalent mass density of the tire with respect to the volume of the rim). The elastic effect of each tire is modeled by using a P-C beam element with its axial stiffness *k* determined by $k = F/\delta$, where *F* denotes the vertical load on a wheel and δ is the vertical deflection of the tire. (v) The "spring-damper unit" in the front or rear suspension mechanism is modeled by using a P-P beam element with its axial stiffness *k* determined by the similar way like that of the tire.

For the dynamic analysis, the main objective of this paper is to investigate the influence of the next parameters on the free vibration characteristics (such as natural frequencies and mode shapes) of the bike: (i) the masses of the attachments; (ii) the radius of hub (disks); (iii) the pretension of each spoke; (iv) the mass (and riding gesture) of the rider. For the static analysis, the influence of the last parameters on the deformations and internal forces (and bending moments) of any structural members may be studied. However, to save space, only the influence of the mass (and riding gesture) of the rider on those of some pertinent members is studied.

II. FORMULATIONS OF THE PROBLEM

The equation of motion for the free vibrations of an un-damped structural system is to take the form, $[m]\{\ddot{u}\}+[k]\{u\}=0$, where $[m]$ is the overall mass matrix, $[k]$ is the overall stiffness matrix, $\{u\}$ is the overall displacement vector and $\{\ddot{u}\}$ is the associated acceleration vector. Thus, the information required for constructing the matrices $[k]$ and $[m]$ are presented in this section.

2.1 Stiffness and mass matrices for the three kinds of beam elements

The three kinds of beam elements adopted in this paper are shown in Fig. 1. Each element has two nodes represented by ① and ②, respectively. Fig. 1(a) shows the pinned-pinned (P-P) beam element, there are two degrees of freedom (dof's) at each node. The force-displacement relationship for this P-P beam element is given by [9]

$$\{S\}_{PP} = [k]_{PP}\{u\}_{PP} \tag{1}$$

where

$$\{S\}_{PP} = [S_1 \quad S_2 \quad S_3 \quad S_4]^T \tag{2a}$$

$$\{u\}_{PP} = [u_1 \quad u_2 \quad u_3 \quad u_4]^T \tag{2b}$$

$$[k]_{PP} = \left[\begin{array}{cc:cc} k_{11} & k_{12} & k_{13} & k_{14} \\ k_{21} & k_{22} & k_{23} & k_{24} \\ \hdashline k_{31} & k_{32} & k_{33} & k_{34} \\ k_{41} & k_{42} & k_{43} & k_{44} \end{array}\right] \tag{2c}$$

In the above expressions, $\{S\}_{PP}$ and $\{u\}_{PP}$ represent the node force vector and node displacement vector of the P-P beam element, respectively, and $[k]_{PP}$ is the corresponding stiffness matrix with its coefficients given by Eq. (A.1) in Appendix A. Furthermore, the symbols ρ, *E*, *A* and ℓ appearing in Fig. 1(a) represent mass density, Young's modulus, cross-sectional area and length of the beam element, respectively.

Fig. 1(b) shows the pinned-clamped (P-C) beam element, there are two dof's at node ① and three dof's at node ②. The force-displacement relationship for this P-C beam element is given by [10]

$$\{S\}_{PC} = [k]_{PC}\{u\}_{PC} \tag{3}$$

where

$$\{S\}_{PC} = [S_1 \quad S_2 \quad S_3 \quad S_4 \quad S_5]^T \tag{4a}$$

$$\{u\}_{PC} = [u_1 \quad u_2 \quad u_3 \quad u_4 \quad u_5]^T \tag{4b}$$

$$[k]_{PC} = \left[\begin{array}{cc:ccc} k_{11} & k_{12} & k_{13} & k_{14} & k_{15} \\ k_{21} & k_{22} & k_{23} & k_{24} & k_{25} \\ \hdashline k_{31} & k_{32} & k_{33} & k_{34} & k_{35} \\ k_{41} & k_{42} & k_{43} & k_{44} & k_{45} \\ k_{51} & k_{52} & k_{53} & k_{54} & k_{55} \end{array}\right] \tag{4c}$$

where $\{S\}_{PC}$, $\{u\}_{PC}$ and $[k]_{PC}$ represent the force vector, displacement vector and stiffness matrix of the P-C beam element, respectively, and the coefficients for $[k]_{PC}$ is given by Eq. (A.3). In addition to the symbols, ρ, *E*, *A* and ℓ, have been defined previously, the other symbol appearing in Fig. 1(b), *I*, represents the moment of inertia of the cross-sectional area *A*.

Fig. 1(c) shows the clamped-clamped (C-C) beam element, there are three dof's at each node. The force-displacement relationship for this C-C beam element is given by [9]

$$\{S\}_{CC} = [k]_{CC}\{u\}_{CC} \tag{5}$$

where

$$\{S\}_{CC} = [S_1 \quad S_2 \quad S_3 \quad S_4 \quad S_5 \quad S_6]^T \tag{6a}$$

$$\{u\}_{CC} = [u_1 \quad u_2 \quad u_3 \quad u_4 \quad u_5 \quad u_6]^T \tag{6b}$$

$$[k]_{CC} = \left[\begin{array}{ccc:ccc} k_{11} & k_{12} & k_{13} & k_{14} & k_{15} & k_{16} \\ k_{21} & k_{22} & k_{23} & k_{24} & k_{25} & k_{26} \\ k_{31} & k_{32} & k_{33} & k_{34} & k_{35} & k_{36} \\ \hdashline k_{41} & k_{42} & k_{43} & k_{44} & k_{45} & k_{46} \\ k_{51} & k_{52} & k_{53} & k_{54} & k_{55} & k_{56} \\ k_{61} & k_{62} & k_{63} & k_{64} & k_{65} & k_{66} \end{array}\right] \tag{6c}$$

Where $\{S\}_{CC}$, $\{u\}_{CC}$ and $[k]_{CC}$ represent the force vector, displacement vector and stiffness matrix of the C-C beam element, respectively, and the coefficients of $[k]_{CC}$ is given by Eq. (A.5).

In addition to the above-mentioned stiffness matrices defined by Eqs. (A.1), (A.3) and (A.5), free vibration analysis of a structural system also requires the mass matrix for each of the constituent members. The mass matrices, $[m]_{PP}$, $[m]_{PC}$ and $[m]_{CC}$, for the P-P, P-C and C-C beam elements are given by Eqs. (A.2), (A.4) and (A.6) in Appendix A, respectively.

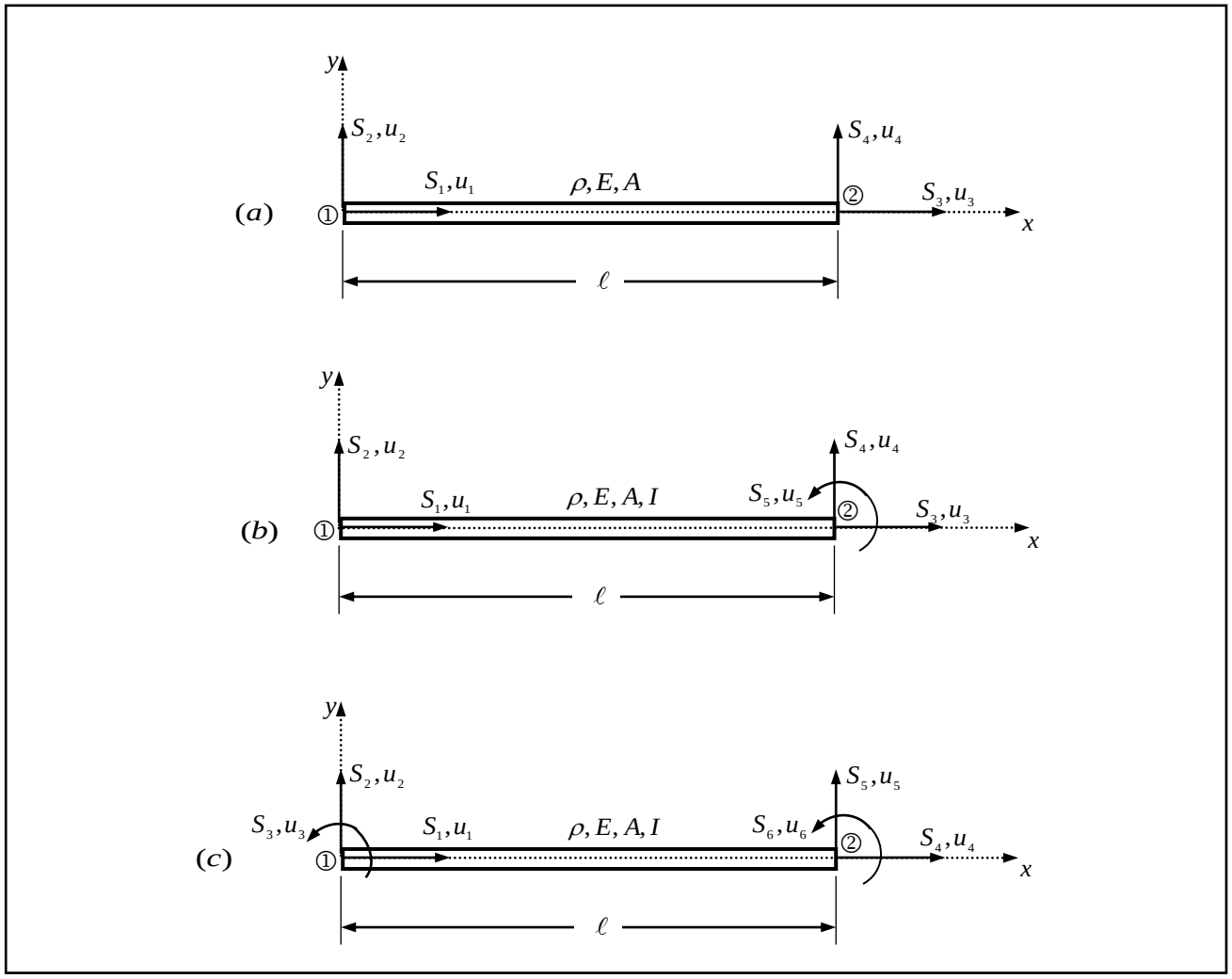

FIG. 1 THE THREE KINDS OF TWO-NODE BEAM ELEMENTS ADOPTED IN THIS PAPER: (*a*) P-P, (*b*) P-C AND (*c*) C-C BEAM ELEMENTS

2.2 Transformation matrices for the three kinds of beam elements

The element stiffness matrix $[k]_q$ and mass matrix $[m]_q$ (q = PP, PC or CC) introduced in the last subsection are obtained with respect to the local coordinate system *xy*. In the conventional FEM, the overall stiffness matrix $[\overline{K}]$ and mass matrix $[\overline{M}]$ are obtained from the element stiffness matrix $[\overline{k}]_q$ and mass matrix $[\overline{m}]_q$ for each of the structural members composed of the entire structure, by using the numerical assembly technique. Where $[\overline{k}]_q$ and $[\overline{m}]_q$ are the property matrices with respect to the global coordinate system $\overline{x}\overline{y}$. In other words, each element stiffness matrix $[k]_q$ and mass matrix $[m]_q$ must be transformed into $[\overline{k}]_q$ and $[\overline{m}]_q$ by using the following formulas

$$[\bar{k}]_q = [\lambda]_q^T [k]_q [\lambda]_q \tag{7a}$$

$$[\bar{m}]_q = [\lambda]_q^T [m]_q [\lambda]_q \tag{7b}$$

then they may be used for assembly.

In Eq. (7), the symbol $[\lambda]_q$ denotes the transformation matrix for the *q*-type beam element. For the P-P beam element as shown in Fig. 2, its node displacements with respect the local *xy* coordinate system, u_i $(i=1-4)$, and the corresponding ones with respect to the global $\bar{x}\bar{y}$ coordinate system, $\bar{u}_i$ $(i=1-4)$, have the following relationship

$$\{u\}_{PP} = [\lambda]_{PP} \{\bar{u}\}_{PP} \tag{8}$$

where $\{u\} = [u_1 \quad u_2 \quad u_3 \quad u_4]^T$ and $\{\bar{u}\} = [\bar{u}_1 \quad \bar{u}_2 \quad \bar{u}_3 \quad \bar{u}_4]^T$ represent the displacement vectors with respect to the local *xy* and global $\bar{x}\bar{y}$ coordinate systems, respectively, while $[\lambda]_{PP}$ is the transformation matrix of the P-P beam element given by [9]

$$[\lambda]_{PP} = \left[\begin{array}{cc:cc} \nu & \mu & 0 & 0 \\ -\mu & \nu & 0 & 0 \\ \hdashline 0 & 0 & \nu & \mu \\ 0 & 0 & -\mu & \nu \end{array}\right] \tag{9}$$

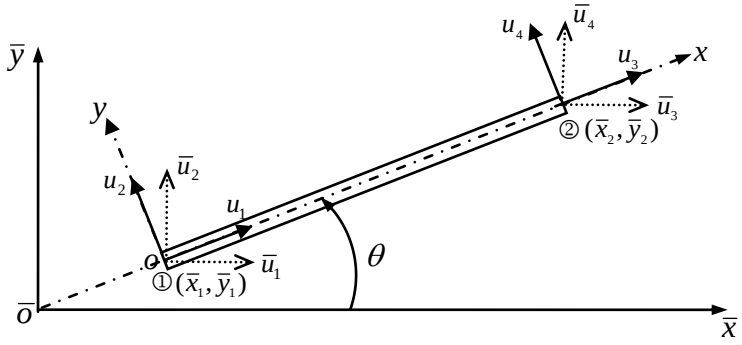

FIG. 2 THE NODE DISPLACEMENTS OF A P-P BEAM ELEMENT WITH RESPECT TO THE LOCAL *xy* COORDINATE SYSTEM, u_i $(i=1-4)$, AND THE CORRESPONDING ONES WITH RESPECT TO THE GLOBAL $\bar{x}\bar{y}$ COORDINATE SYSTEM $\bar{u}_i$ $(i=1-4)$.

where

$$\nu = \cos\theta, \quad \mu = \sin\theta \tag{10a,b}$$

In the last expressions, θ is the angle between positive *x*-axis and positive $\bar{x}$-axis as one may see from Fig. 2. In practice, the values of ν and μ are determined by

$$\nu = \frac{\bar{x}_2 - \bar{x}_1}{\sqrt{(\bar{x}_2 - \bar{x}_1)^2 + (\bar{y}_2 - \bar{y}_1)^2}} \tag{11a}$$

$$\mu = \frac{\bar{y}_2 - \bar{y}_1}{\sqrt{(\bar{x}_2 - \bar{x}_1)^2 + (\bar{y}_2 - \bar{y}_1)^2}} \tag{11b}$$

where $(\bar{x}_1, \bar{y}_1)$ and $(\bar{x}_2, \bar{y}_2)$ are the global coordinates of node ① and node ② of the beam element as shown in Fig. 2, respectively.

Similarly, the transformation matrix for the P-C beam element is given by [10]

$$[\lambda]_{PC} = \left[\begin{array}{cc:ccc} \nu & \mu & 0 & 0 & 0 \\ -\mu & \nu & 0 & 0 & 0 \\ \hdashline 0 & 0 & \nu & \mu & 0 \\ 0 & 0 & -\mu & \nu & 0 \\ 0 & 0 & 0 & 0 & 1 \end{array}\right] \tag{12}$$

and the transformation matrix for the C-C beam element is given by [9]

$$[\lambda]_{CC} = \left[\begin{array}{ccc:ccc} \nu & \mu & 0 & 0 & 0 & 0 \\ -\mu & \nu & 0 & 0 & 0 & 0 \\ 0 & 0 & 1 & 0 & 0 & 0 \\ \hdashline 0 & 0 & 0 & \nu & \mu & 0 \\ 0 & 0 & 0 & -\mu & \nu & 0 \\ 0 & 0 & 0 & 0 & 0 & 1 \end{array}\right] \tag{13}$$

2.3 Geometric stiffness matrices for various beam elements

In order to investigate the effect of pretension T_s in each of the spokes on the free vibration characteristics of a bike, the geometric stiffness matrix $[k_G]_q$ for the relevant beam elements are presented in this subsection [12].

For a spoke modeled by using the P-P beam element, the pretension T_s in it will increase its axial stiffness. Thus, its geometric stiffness $[k_G]_{PP}$ is given by

$$[k_G]_{PP} = \left[\begin{array}{cc:cc} T_s/\ell_s & 0 & -T_s/\ell_s & 0 \\ 0 & 0 & 0 & 0 \\ \hdashline -T_s/\ell_s & 0 & T_s/\ell_s & 0 \\ 0 & 0 & 0 & 0 \end{array}\right] \tag{14}$$

where ℓ_s represents the length of each spoke.

For a spoke modeled by using the P-C beam element, the pretension T_s in it will increase its stiffness associated with both the axial dof's and transverse dof's. Thus, its geometric stiffness $[k_G]_{PC}$ is given by

$$[k_G]_{PC} = \left[\begin{array}{ccc:cc} T_s/\ell_s & 0 & & -T_s/\ell_s & 0 & 0 \\ 0 & T_s/\ell_s & & 0 & -T_s/\ell_s & 0 \\ \hdashline -T_s/\ell_s & 0 & & T_s/\ell_s & 0 & 0 \\ 0 & -T_s/\ell_s & & 0 & T_s/\ell_s & 0 \\ 0 & 0 & & 0 & 0 & 0 \end{array}\right] \tag{15}$$

From Fig. 1(b) one sees that, for a P-C beam element, its 1st and 3rd dof's are in the axial direction, and its 2nd and 4th dof's are in the transverse direction, thus, in Eq. (15), the matrix coefficients $k_{G,mn}$ with $m,n = 1$ or 3 represent the contribution of pretension T_s to the stiffness of axial dof's, and those with $m,n = 2$ or 4 represent the contribution of pretension T_s to the stiffness of transverse dof's of the P-C beam elements. Furthermore, since the pretension does not affect the stiffness of rotational dof's with displacement u_5 (cf. Fig. 1(b)), the matrix coefficients $k_{G,m5}$ and $k_{G,5n}$ with $m,n = 1-5$ are equal to zero in Eq. (15).

When there exists pretension T_s in each spoke, the front or rear rim will subjected to the compressive force T_r. Since the rim is modeled by a number of C-C beam elements, the geometric matrix $[k_G]_{CC}$ for each of the rim elements is given by

$$[k_G]_{CC} = \left[\begin{array}{ccc:ccc} -T_r/\ell_r & 0 & 0 & T_r/\ell_r & 0 & 0 \\ 0 & -T_r/\ell_r & 0 & 0 & T_r/\ell_r & 0 \\ 0 & 0 & 0 & 0 & 0 & 0 \\ \hdashline T_r/\ell_r & 0 & 0 & -T_r/\ell_r & 0 & 0 \\ 0 & T_r/\ell_r & 0 & 0 & -T_r/\ell_r & 0 \\ 0 & 0 & 0 & 0 & 0 & 0 \end{array}\right] \tag{16}$$

where ℓ_r represents the length of each rim element. It is noted that, in Eq. (16), all diagonal coefficients are "negative" and all off-diagonal ones are "positive". This result is opposite to Eqs. (14) and (15), because T_s in Eqs. (14) and (15) is a tensile force and T_r in Eq. (16) is a compressive force. Furthermore, for a C-C beam element as shown in Fig. 1(c), its 3rd displacement u_3 and 6th displacement u_6 belong to the rotational dof's, the associated matrix coefficients in Eq. (16) are equal to zero, i.e., $k_{G,m3} = k_{G,m6} = 0$ for $m = 1-6$ and $k_{G,3n} = k_{G,6n} = 0$ for $n = 1-6$.

2.4 Rim force induced by pretension of spokes

For simplicity, in order to determine the rim force T_r (appearing in Eq. (16)) induced by the pretension of all spokes in a rim, it is assumed that the tensile force T_s in each spoke directs to the center *H* of the hub (cf. Fig. 3). If the total number of spokes is N_s and the average radius of the rim is r_r, then the average central force per unit length of the rim is given by

$$p = \frac{N_s T_s}{2\pi r_r} \tag{17}$$

For the free-body diagram of the half rim shown in Fig. 3, the force equilibrium in *y*-direction requires that

$$\int_0^{2\pi} pr_r \sin\theta d\theta = 2T_r \tag{18}$$

From Eqs. (17) and (18) one obtains

$$T_r = pr_r = \frac{N_s T_s}{2\pi} \tag{19}$$

For the present paper, the total number of spokes in each rim is $N_s = 36$, it is seen that $T_r / T_s = 5.73$ according to Eq. (19). If the pretension T_s in the spokes is considered as the "distributed" load, then the compressive force T_r in the rim is equivalent to the "concentrated" load. In general, the effect of "distributed" load is much less than the "concentrated" load if the summation magnitude of the former is equal to the magnitude of latter. Since the effect of pretension T_s is to raise the stiffness of spokes and that of compressive force T_r is to reduce the stiffness of the rim, it is evident that the overall effect of increasing the pretension T_s will reduce the overall stiffness of the sub-structural system composed of hub (disk), spokes and rim. This is the reason why the lowest several natural frequencies of the bike decrease with the increase of pretension T_s as one may see from the subsequent numerical examples.

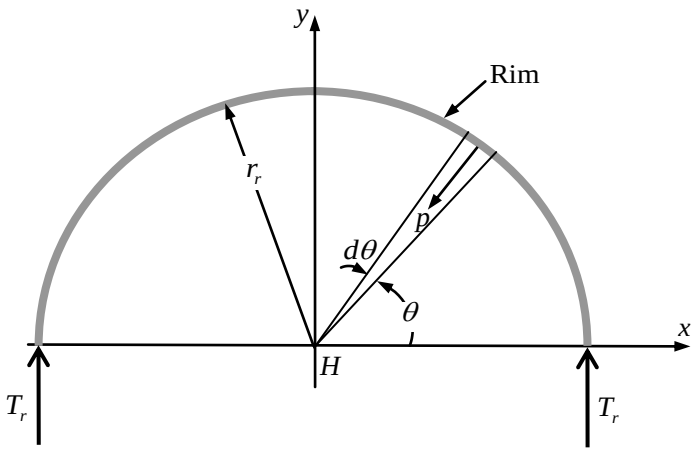

FIG. 3 FREE-BODY DIAGRAM OF THE HALF RIM SUBJECTED TO UNIFORM CENTRAL FORCE p PER UNIT LENGTH

2.5 Global coordinates for the two nodes of each spoke

In the finite element analysis, preparation of input data is one of the heaviest tasks. For the bike studied in this paper, the total number of spokes in each wheel is $N_s = 36$. Thus, according to Eqs. (11a) and (11b), one must input the computer 72 pairs of data concerning the global coordinates of the two nodes ① and ② of each spoke, ($\bar{x}_1$, $\bar{y}_1$) and ($\bar{x}_2$, $\bar{y}_2$), then one can obtain the transformation matrix $[\lambda]_q$ of all spokes. For simplicity, the technique for determining the values of ($\bar{x}_1$, $\bar{y}_1$) and ($\bar{x}_2$, $\bar{y}_2$) are presented in this subsection.

For the 36 spokes in each wheel, each of them is modeled by a two-node P-P beam element. The 1st node ① of each spoke is located on the rim, however, the 2nd nodes ② for one half of the 36 spokes are on the 1st (hub) disk and those for the other half of the 36 spokes are on the 2nd (hub) disk as shown in Fig. 4 and Table 1. Because the 36 nodes are uniformly distributed on the rim (or hub disks), the subtended angle between any two adjacent nodes is given by $\Delta\theta = 360° / N_s = 10°$.

For convenience, the 36 nodes on the rim (or hub disks) are denoted by 1, 2, …, 36 and the associated spokes by (1), (2), …, (36), respectively, beginning from $\theta_i = 0$ (or $\theta_j = 0$) as one may see from Fig. 4. It is noted that the numbering for node ① (on the rim) of *i*-th spoke is *i*, however, the numbering for node ② (on the hub disks) of the same *i*-th spoke is *j* as shown in Table 1. From Table 1, one sees that the 2nd nodes ② of the spokes with "odd" numberings are on (hub) disk 1 and those with "even" numberings are on (hub) disk 2, and, in Fig. 4, the odd numbering spokes are denoted by the solid lines (——) and the even numbering spokes by the dashed lines (------).

Based on the last descriptions and Fig. 4, the global coordinates for the two nodes of the arbitrary *i*-th spoke are given by

$$\bar{x}_{1,i} = \bar{x}_h - r_r \cos\theta_{1,i}\,,\ \bar{y}_{1,i} = \bar{y}_h + r_r \sin\theta_{1,i} \qquad \text{(for node ①)} \tag{20a}$$

$$\bar{x}_{2,i} = \bar{x}_h - r_h \cos\theta_{2,i}\,,\ \ \bar{y}_{2,i} = \bar{y}_h + r_h \sin\theta_{2,i} \qquad \text{(for node ②)} \tag{20b}$$

with

$$\theta_{1,i} = (i-1)\Delta\theta \tag{21a}$$

$$\theta_{2,i} = (j-1)\Delta\theta \tag{21b}$$

$$\Delta\theta = 2\pi / N_s \tag{21c}$$

where $(\bar{x}_h\,, \bar{y}_h)$ are the global coordinates of hub center *H*, r_r and r_h are the radii of the rim and the hub disks, respectively, while $\theta_{1,i}$ and $\theta_{2,i}$ are the angles between the radii at nodes ① and ② and the "negative" $\bar{x}$-axis, respectively. From Eqs. (20a) and (20b), one sees that $\bar{x}_{2,i} = \bar{x}_h$ and $\bar{y}_{2,i} = \bar{y}_h$ if the radius of the hub disks is very small so that $r_h \approx 0$.

Since the stiffness of the hub (disk) is much greater than that of each of the spokes, it is reasonable to assume that the hub (disk) is a "rigid body", for simplicity. Furthermore, since the bike wheel is to rotate about its central axle, the center of the hub must be pinned. Based on the last assumptions, the translational displacements of node ② of any *i*-th spoke are identical to those of the hub center *H*, i.e.,

$$\bar{u}_{3,i} = \bar{u}_{x,h} \tag{22a}$$

$$\bar{u}_{4,i} = \bar{u}_{y,h} \tag{22b}$$

Eqs. (22a) and (22b) mean that the "numberings" for the degrees of freedom of 2nd node ② of each spoke are the same as those of the hub center *H*. However, the global coordinates $(\bar{x}_{2,i}\,, \bar{y}_{2,i})$ given by Eq. (20b) required for the determination of the transformation matrix $[\lambda]_i$ of the *i*-th spoke are different from each other for each of the spokes.

From Fig. 4 one sees that the "moment arm" for the tensile force in each spoke with respect to the hub center *H* increases with the increase of radius r_h of the hub disk, so does the restoring moment induced by the spoke tension. Thus, the effective stiffness of the sub-structural system composed of the rim, spokes and hub (disks) increases with the increase of r_h, this is the reason why the lowest several natural frequencies of the entire bike structure increase with the increase of r_h as one may see from the numerical examples given in the latter section 5.

TABLE 1

THE NUMBERINGS FOR NODES ① AND ② OF EACH SPOKE I ($i = 1-36$) IN A RIM.

Spokes (i)		19	20	21	22	23	24	25	26	27	28	29	30	31	32	33	34	35	36
Node ① (i)		19	20	21	22	23	24	25	26	27	28	29	30	31	32	33	34	35	36
Node ② (j)	*Odd	**13**		**27**		**17**		**31**		**21**		**35**		**25**		**3**		**29**	
	*Even		**26**		**16**		**30**		**20**		**34**		**24**		**2**		**28**		**6**

Spokes (i)		1	2	3	4	5	6	7	8	9	10	11	12	13	14	15	16	17	18
Node ① (i)		1	2	3	4	5	6	7	8	9	10	11	12	13	14	15	16	17	18
Node ② (j)	*Odd	**7**		**33**		**11**		**1**		**15**		**5**		**19**		**9**		**23**	
	*Even		**32**		**10**		**36**		**14**		**4**		**18**		**8**		**22**		**12**

Note: The 2nd nodes ② for the spokes with "odd" numberings are on hub disk 1 and those with "even" numberings are on hub disk 2 (cf. Fig. 4).

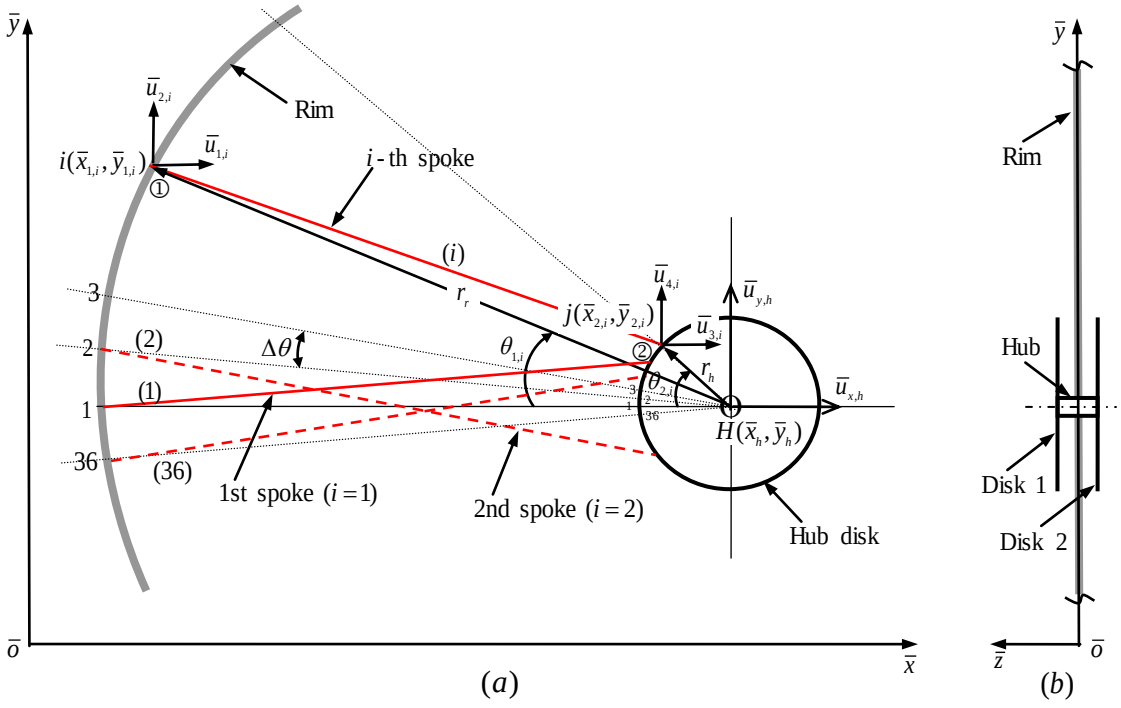

FIG.4 (a) SIDE VIEW AND (b) FRONT VIEW OF THE BIKE WHEEL "WITH HUB PINNED". THE COORDINATES OF THE 2ND NODE ② OF THE i TH SPOKE ON THE RIGID HUB DISK ARE GIVEN BY $\bar{x}_{2,i} = \bar{x}_h - r_h \cos\theta_{2,i}$ AND $\bar{y}_{2,i} = \bar{y}_h + r_h \sin\theta_{2,i}$ WITH $\theta_{2,i}$ DENOTING THE ANGLE BETWEEN THE RADIUS r_h OF THE HUB DISK H AT NODE ② AND THE "NEGATIVE" $\bar{x}$ -AXIS.

III. NATURAL FREQUENCIES AND MODE SHAPES OF THE BIKE

Based on the stiffness matrix $[k]_q$, mass matrix $[m]_q$, geometric stiffness matrix $[k_G]_q$ and the transformation matrix $[\lambda]_q$, one may obtained the property matrices of various beam elements with respect to the global coordinates and assembly of the latter will define the equation of motion of the entire bike structure

$$[\overline{M}]_{\overline{N}\times\overline{N}}\{\ddot{\overline{u}}\}_{\overline{N}\times 1}+[\overline{K}]_{\overline{N}\times\overline{N}}\{\overline{u}\}_{\overline{N}\times 1}=0 \tag{23a}$$

After imposing the boundary conditions with all the constrained dof's eliminated, one obtains

$$[\widetilde{M}]_{\widetilde{N}\times\widetilde{N}}\{\ddot{\widetilde{u}}\}_{\widetilde{N}\times 1}+[\widetilde{K}]_{\widetilde{N}\times\widetilde{N}}\{\widetilde{u}\}_{\widetilde{N}\times 1}=0 \tag{23b}$$

In the above two equations, $[\overline{M}]$ (or $[\widetilde{M}]$) is the overall mass matrix, $[\overline{K}]$ (or $[\widetilde{K}]$) is the overall stiffness matrix, $[\overline{u}]$ (or $[\widetilde{u}]$) is the overall displacement vector and $[\ddot{\overline{u}}]$ (or $[\ddot{\widetilde{u}}]$) is the overall acceleration vector. Furthermore, $\overline{N}$ and $\widetilde{N}$ are the total dof's (including unconstrained and constrained ones) and the total unconstrained dof's, respectively.

For free vibrations, one has

$$\{\overline{u}(t)\}=\{\overline{U}\}e^{i\omega t} \tag{24}$$

where $\{\overline{U}\}$ is the amplitude of $\{\overline{u}(t)\}$, ω (rad/sec) is the natural frequency of the vibrating system and $i=\sqrt{-1}$.

Substituting Eq. (24) into Eq. (23a) leads to

$$([\overline{K}]-\omega^2[\overline{M}])\{\overline{U}\}=0 \tag{25a}$$

Similarly, from Eq. (23b) one may obtain

$$([\widetilde{K}]-\omega^2[\widetilde{M}])\{\widetilde{U}\}=0 \tag{25b}$$

Eq. (25a) or (25b) is a standard characteristic equation, from which one may determine the *r*-th natural frequency ω_r and the corresponding mode shape $\{\overline{U}\}_r$ (or $\{\widetilde{U}\}_r$), $r=1,2,3,\ldots$, of the vibrating system. In this paper, the Jacobi method [13] is used to solve Eq. (25), and the rth mode shape is determined by using the following global coordinates of all nodes

$$\widetilde{X}_i^{(r)}=\overline{x}_i+\widetilde{U}_{xi}^{(r)}\ (i=1-n_n) \tag{26a}$$

$$\widetilde{Y}_i^{(r)}=\overline{y}_i+\widetilde{U}_{yi}^{(r)}\ (i=1-n_n) \tag{26b}$$

where ($\overline{x}_i$, $\overline{y}_i$) are global coordinates of node i required for the determination of transformation matrix $[\lambda]_q$ of the associated beam element as one may see from Eq. (11), $\widetilde{U}_{xi}^{(r)}$ and $\widetilde{U}_{yi}^{(r)}$ are displacement components of node i in the $\overline{x}$ and $\overline{y}$ directions, respectively, and n_n is the total number of nodes of the entire vibrating system. It is noted that $\widetilde{U}_{xi}^{(r)}$ and $\widetilde{U}_{yi}^{(r)}$ are parts of the components of the *r*-th mode shape $\{\widetilde{U}\}_r$ determined from Eq. (25b), and the displacement components of the "constrained" dof's are equal to zero. In this paper, the original configuration of the bike is obtained from the global coordinates ($\overline{x}_i$, $\overline{y}_i$) with $i=1-n_n$ and the r-th mode shape is obtained from the global coordinates ($\widetilde{X}_i^{(r)}$, $\widetilde{Y}_i^{(r)}$) with $i=1-n_n$.

IV. REACTIVE FORCES AND MEMBER FORCES

For a static "constrained" structural system, its force-displacement relationship is given by

$$[\widetilde{K}]\{\widetilde{u}\} = \{\widetilde{F}\} \tag{27}$$

where $[\widetilde{K}]$ and $\{\widetilde{u}\}$ have been defined in Eq. (23b), and $\{\widetilde{F}\}$ is the associated external force vector. Once the external load $\{\widetilde{F}\}$ is given, then from Eq. (27) one may obtain the node displacement vector

$$\{\widetilde{u}\} = [\widetilde{K}]^{-1}\{\widetilde{F}\} \tag{28}$$

If the *i*-th dof of the structural system is constrained, then the associated reactive force (or moment) is determined by

$$\hat{R}_i = \sum_{j=1}^{\bar{N}} \bar{k}_{ij}\hat{u}_j \tag{29}$$

where $\bar{k}_{ij}$ are the matrix coefficients of the unconstrained stiffness matrix $[\bar{K}]_{\bar{N}\times\bar{N}}$ defined by Eq. (23a), $\hat{u}_j$ are components of the displacement vector $\{\hat{u}\}_{\bar{N}\times 1}$ composed of the non-zero components $\{\widetilde{u}\}_{\tilde{N}\times 1}$ given by Eq. (28) and the zero components corresponding to the "constrained" dof's. The reactive forces $\hat{R}_i$ obtained from Eq. (29) are with respect to the global $\bar{x}\bar{y}$ coordinate system.

Based on the node displacement vector $\{\hat{u}\}_{\bar{N}\times 1}$, one may obtained the node force vector $\{\hat{F}\}^{(s)}$ of the *s*-th member (or beam element) with respect to the global $\bar{x}\bar{y}$ coordinate system

$$\{\hat{F}\}^{(s)} = [\bar{k}]^{(s)}\{\hat{u}\}^{(s)} \tag{30}$$

where $[\bar{k}]^{(s)}$ and $\{\hat{u}\}^{(s)}$ are the stiffness matrix and displacement vector of the *s*-th beam element. The former $[\bar{k}]^{(s)}$ has been determined before it is used to assemble the overall stiffness matrix $[\bar{K}]_{\bar{N}\times\bar{N}}$ and the latter $\{\hat{u}\}^{(s)}$ is part of the components of $\{\hat{u}\}_{\bar{N}\times 1}$. In structural design, one requires the force vector $\{F\}^{(s)}$ of the *s*-th member with respect to the local xy coordinate system. In such a case, the values of $\{F\}^{(s)}$ may be obtained from

$$\{F\}^{(s)} = [\lambda]^{(s)}\{\hat{F}\}^{(s)} \tag{31}$$

where $[\lambda]^{(s)}$ is the transformation matrix of the *s*-th beam element.

V. NUMERICAL RESULTS AND DISCUSSIONS

The finite element model studied in this paper is shown in Fig. 5. For convenience, the entire bike is subdivided into three subsystems: the bike body, the front wheel and the rear wheel. The bike body is composed of 40 beam elements connected by 35 nodes, either front wheel or rear wheel is composed of 36 spokes, 36 rim elements, one tire and one hub. The diameter of each spoke is 2 mm and is modeled by a two-node pinned-pinned (P-P) beam element. The approximate cross-section of each rim is to take the form as shown in Fig. 6, its sectional area is $A_r = 60.61\,\text{mm}^2$, moment of inertia of A_r about its neutral axis n-n is $I_r = 1362.3259\,\text{mm}^4$, the average radius of rim (based on the neutral axis *n*-*n*) is $r_r = 277.5\,\text{mm}$ (cf. Fig. 6), each rim element is modeled by a clamped-clamped (C-C) beam element. The mass of each tire is assumed to uniformly distribute along the circumference of the attached rim and combined with the rim so that the effective mass density of the rim is given by $\bar{\rho}_r = \rho_{\text{rim}} + \bar{\rho}_{\text{tire}}$, where $\rho_{\text{rim}} = 7850\,\text{kg}/\text{m}^3$ is the mass density of the rim material itself and $\bar{\rho}_{\text{tire}}$ is the equivalent mass density of the tire with respect to the rim volume and given by $\bar{\rho}_{\text{tire}} = m_t/\forall_{\text{rim}}$ with m_t denoting total mass of each tire and $\forall_{\text{rim}}$ denoting total volume of each rim. For the present example, one has $m_t \approx 1.0\,\text{kg}$ and $\forall_{\text{rim}} \approx 0.10663\times 10^{-3}\,\text{m}^3$, thus, $\bar{\rho}_{\text{tire}} \approx 9378\,\text{kg}/\text{m}^3$. The spring constant for each tire is assumed to be $k_t = W/\delta = 100\times 9.8/0.002 = 4.9\times 10^5\,\text{N/m}$,

where $W = 100 \times 9.8\,\mathrm{N}$ is the weight of a 100 kg rider and $\delta = 0.002\mathrm{m}$ is the deflection of the tire when it is subjected to the load of the rider. For convenience, the stiffness *k* of the spring-damper unit for front or rear suspension system is assumed to be $k = 5.0 \times 10^5\ \mathrm{N/m}$. The outer diameters of various tubes for the bike body are shown in Table 2, for convenience, the thickness of each tube is assumed to be 2.0 mm. The masses of some attachments are shown in Table 3.

From Fig. 5 one sees that the total number of beam elements for the entire (structural) system is 186 and the total number of nodes is 109. Thus, the total degrees of freedom (dof's) is 325 and the total unconstrained dof's is 321 with the final 4 dof's of the two nodes attaching the ground constrained. Besides, unless particularly stated, the numerical results of this paper are based on the assumption that Young's modulus $E = 2.068 \times 10^{11}\ \mathrm{N/m^2}$, mass density of metal materials $\rho = 7850\,\mathrm{kg/m^3}$, and there is no rider on the bike.

TABLE 2
THE OUTER DIAMETERS OF VARIOUS TUBES FOR THE BIKE BODY EACH WITH THICKNESS 2.0 mm

Name of tubes	Outer diameters (mm)
Head tube	22
Headset bearing tube, front fork tubes	34
Top tube	28.5
Down tube	34
Seat tube	28.5
Seat post, seat stay tubes, chain stay tubes	25.4

TABLE 3
THE MASSES OF SOME PARTS

Item	Name of parts	Mass (kg)	Location (Node No.)	Remarks
1	Handlebar	0.4	1	*Mass of rider isn't considered, yet.
2	Saddle	0.5	18	*Mass of rider isn't considered, yet.
3	[a]Chain	0.3/2 = 0.15	23, 34	Uniformly shared by Nodes 23 and 34
4	Front hub and axle	0.7758	35	
5	Rear hub, axle and attached sprockets	1.5758	34	Combined with item 3 for node 34
6	Crank set, pedals and attachments	1.5	23	Combined with item 3 for node 23
7	[b]Two tires	1.0×2	—	Distributed on the associated rims
[c]Summation		7.0516	—	—

[a]The chain mass is assumed to be equally shared by the rear axle and the crank shaft.
[b]The mass of each tire is considered as the distributed mass on the associated rim.
[c]Some of the attachments (e.g., the braking system) are not included.

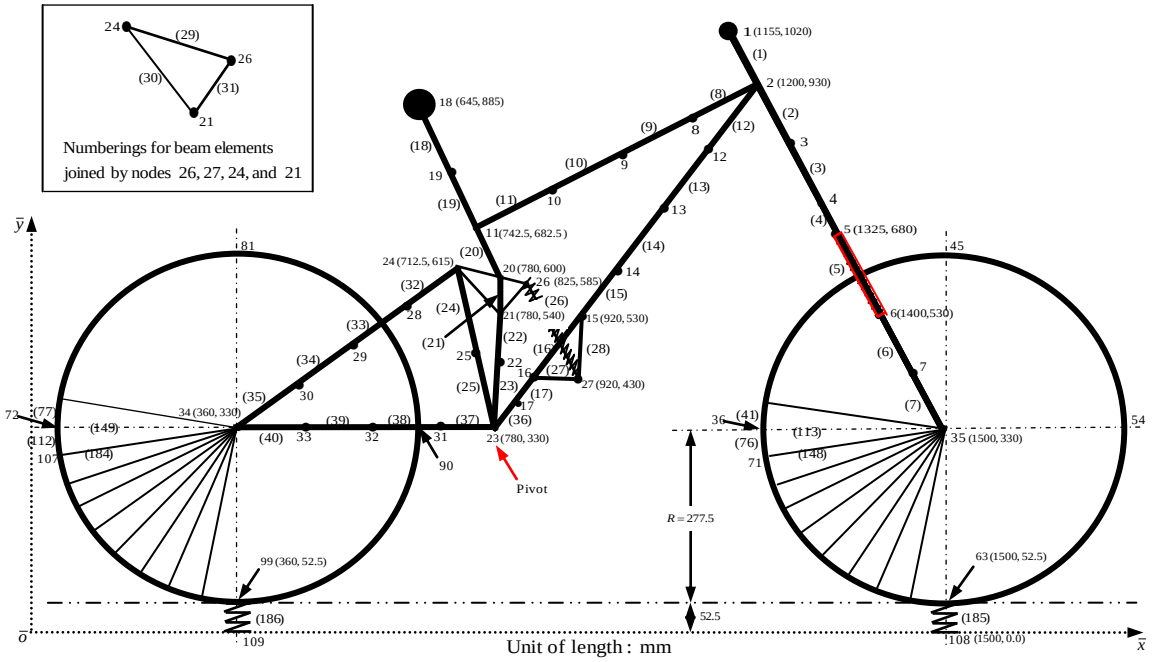

FIG. 5 THE FINITE ELEMENT MODEL OF THE BIKE (WITH $r_h = 0$) STUDIED (CF. FIG. 4 FOR THE CASE WITH $r_h \neq 0$)

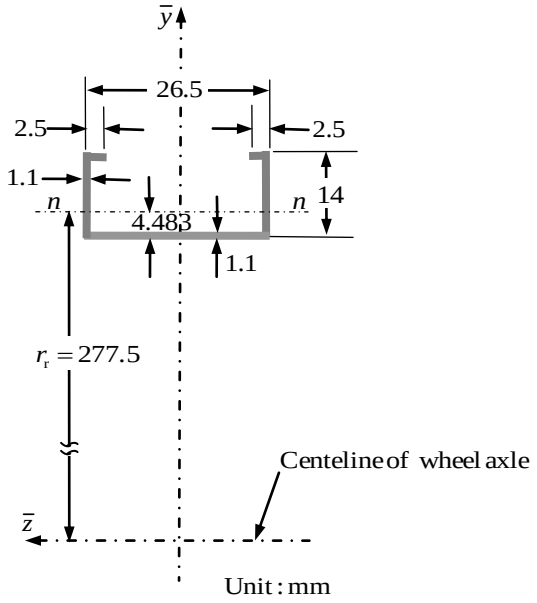

FIG. 6 THE APPROXIMATE CROSS-SECTION OF RIM (UNIFORM THICKNESS: 1.1 mm).

5.1 Influence of attachments

The influence of lumped masses of attachments (as shown in Table 3) on the lowest five natural frequencies of the bike without rider is shown in Table 4. From the table one sees that the lumped masses of attachments (no matter whether masses of the two tires being included or not) significantly affect the lowest five natural frequencies of the bike. This result is under our expectation, because the ratios between the lumped masses of the attachments (or the two tires) and the total mass of the 186 beam elements are high. From Table 3 one sees that the total mass of the attachments (excluding the two tires) is 5.0516

kg, that of the two tires is 2.0 kg, and from the computer output one sees that the total mass of the 186 beam elements is 9.98 kg ($\approx$10 kg). It is seen that the mass ratios of the above-mentioned attachments (or the two tires) to the structural members (contributed to the stiffness of the entire bike) are as high as about 50% (or 20%). For this reason, in the subsequent studies in this paper, the effect of all attachments (including the two tires) as shown in Table 3 are taken into consideration. It is noted that some of the attachments (e.g., the braking system) are not included in Table 3.

TABLE 4
INFLUENCE OF LUMPED MASSES OF ATTACHMENTS ON THE LOWEST FIVE NATURAL FREQUENCIES OF THE BIKE WITHOUT RIDER

Conditions	Natural frequencies, ω_v (rad/sec)				
	ω_1	ω_2	ω_3	ω_4	ω_5
No attachments	223.37730	260.44416	404.32388	455.83124	798.58902
With attachments (including two tires)	168.05399	207.60573	274.94635	311.38074	587.16357
With attachments (excluding two tires)	178.76463	216.50521	302.74445	383.54492	647.78378

5.2 Influence of radius of hub disk

In most of the existing bikes, the radius of hub disk is $r_h \approx 25.0$ mm, therefore, all the numerical results of this paper are based on the last value of r_h. In order to study the influence of r_h on the free vibration characteristics of the bike, four values of r_h are investigated in this subsection: r_h = 25.0, 15.0, 5.0 and 0.0 mm. The lowest five associated natural frequencies are shown in Table 5. From the table one sees that decreasing the radius of hub disk (r_h) will reduce the lowest several natural frequencies of the bike as has been shown in previous subsection 2.5 and the influence is most significant on the 1st natural frequency (ω_1) and decreases with increasing the vibration modes. It is seen that the influence of radius of hub disk (r_h) on the 5th natural frequency (ω_5) is very small so that the corresponding 5th mode shapes for the four values of r_h look similar (cf. Figs. 7(a_5) and (b_5)).

To save the space, only the lowest five mode shapes for r_h = 25.0 and 0.0 mm are shown in Figs. 7($a_1 - a_5$) and ($b_1 - b_5$), respectively. In which, Figs. 7(a_1-a_5) denote the lowest five mode shapes for r_h = 25.0 mm, and Figs. 7(b_1-b_5) denote those for r_h = 0.0 mm. From Fig. 7(a_1) one sees that the 1st mode shape is major in (vertical) up-and-down vibration of the sub-structure in the "rear" suspension system (composed of the seat stays and chain stays) with respect to node 23. This is a reasonable result, because node 23 is a pivot and there exist a linear spring (cf. beam element No. 26 in Fig. 5) with its stiffness ($k = 5.0\times10^5$ N/m) much smaller than the stiffness of the other beam elements in the "rear" suspension system. Figs. 7(a_2) and (a_3) reveal that the 2nd and 3rd mode shapes are major in the heave and pitch motions of the entire bike, respectively. Fig. 7(a_4) reveals that the 4th mode shape is major in (vertical) up-and-down vibration of the sub-structure in the "front" suspension system, this is because there exists a soft linear spring (cf. beam element No. 5 in Fig. 5) in the front fork. The 5th mode shape shown in Fig. 7(a_5) is more complicated, because the vibrations of both the front and rear suspension systems are coupled. It is noted that the 1st natural frequency for r_h = 0.0 mm is near zero ($\omega_1 = 0.00037$

rad/sec) as one may see from Table 5, this leads to the corresponding mode shape shown in Fig. 7(b_1) looking like a rigid-body motion in (horizontal) front-and-back direction.

TABLE 5

INFLUENCE OF RADIUS OF HUB DISK, r_h , ON THE LOWEST FIVE NATURAL FREQUENCIES OF THE BIKE

Radius of hub disk r_h (mm)	Natural frequencies, ω_v (rad/sec)				
	ω_1	ω_2	ω_3	ω_4	ω_5
25.0 (cf. Table 4)	168.05399	207.60573	274.94635	311.38074	587.16357
15.0	105.91116	175.50561	236.21839	282.04038	585.10492
5.0	36.63954	123.17002	226.12836	278.43011	584.15505
0.0	0.00037	114.78185	225.45303	278.07291	583.95400

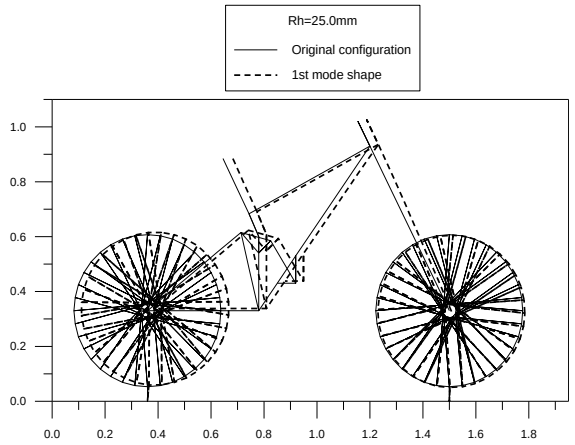

(a_1)

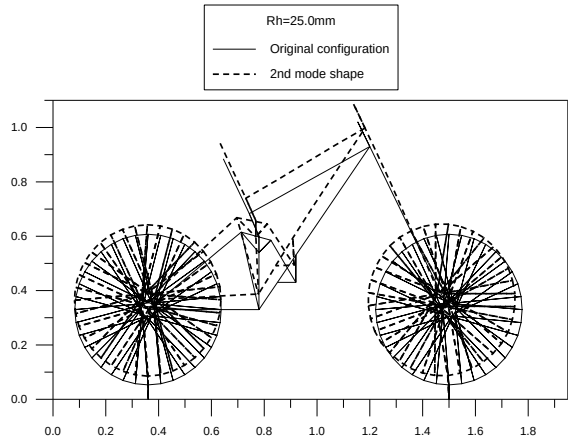

(a_2)

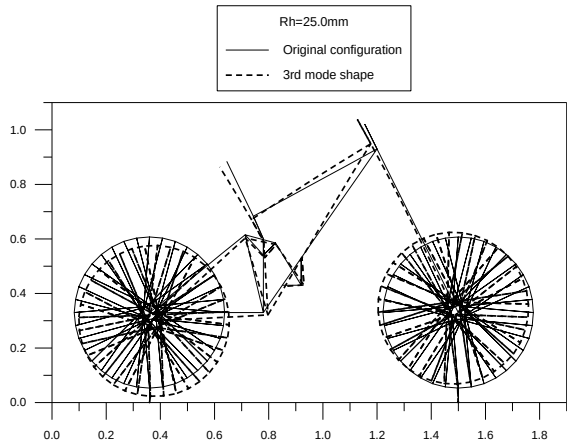

(a_3)

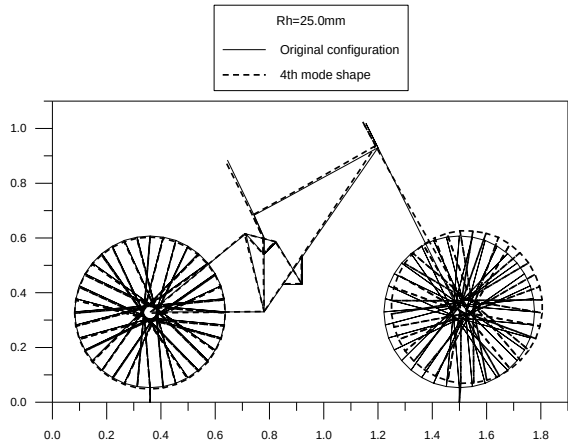

(a_4)

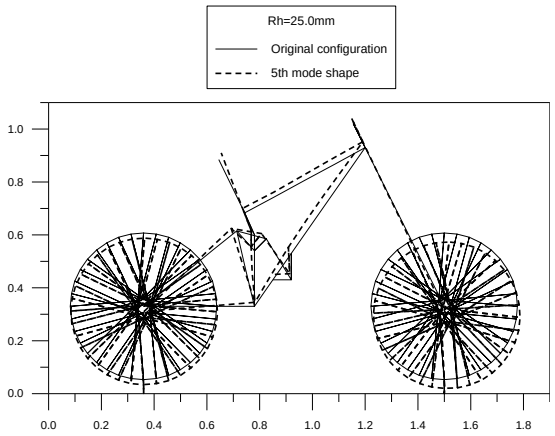

(a_5)

FIG. 7 THE LOWEST FIVE MODE SHAPES OF THE BIKE: ($a_1 - a_5$) FOR $r_h = 25.0$ MM , AND ($b_1 - b_5$) FOR $r_h = 0.0$ MM

.

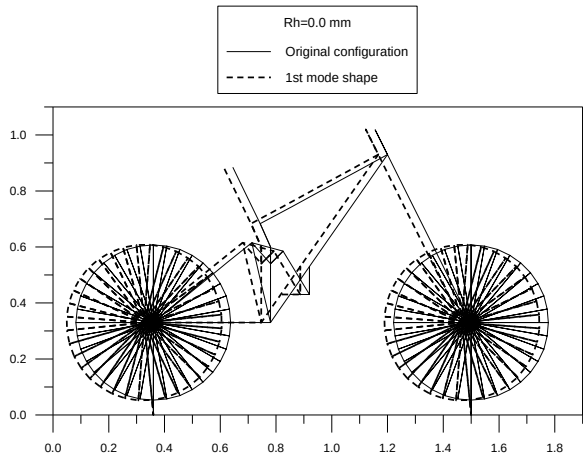

(b_1)

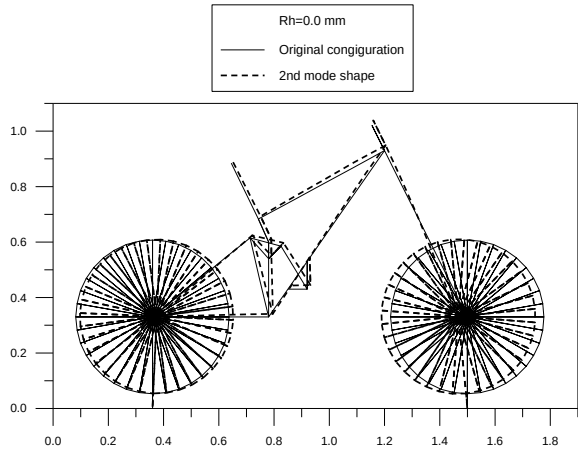

(b_2)

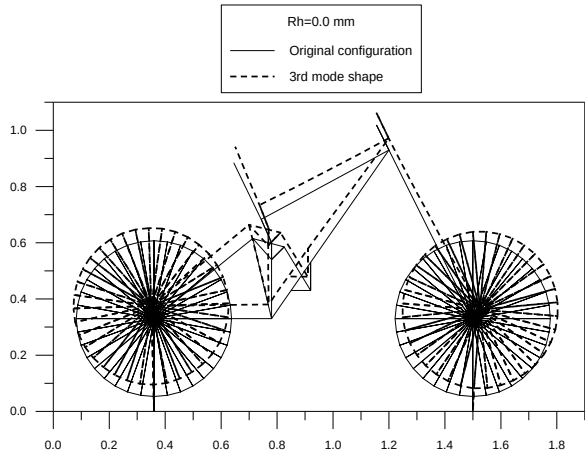

(b_3)

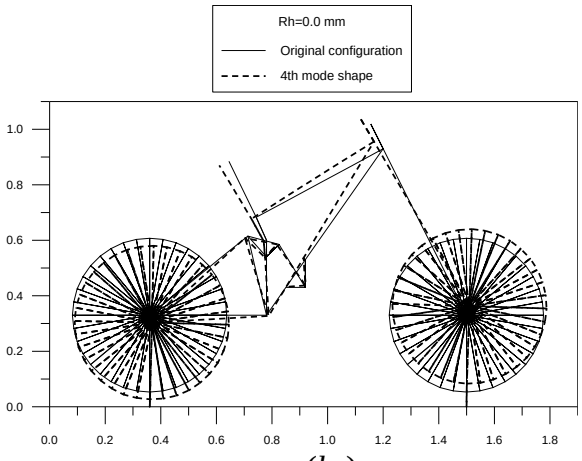

(b_4)

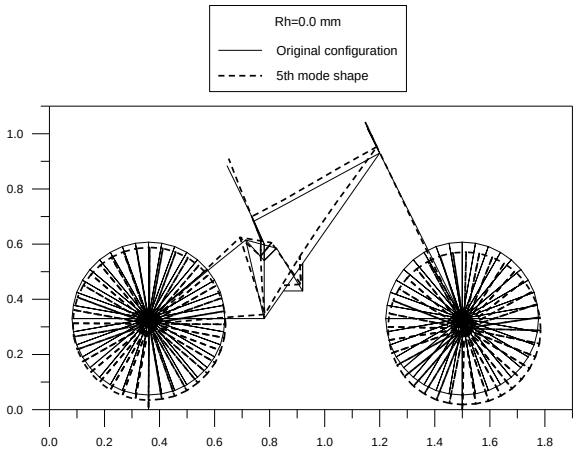

(b_5)

FIG. 7 ($b_1 - b_5$) (CONTINUED)

5.3 Influence of pretension in spokes

A bicycle wheel is composed of rim, hub, spokes and tire. Among the components, the rim and hub are connected together to constitute a strong structure system by relying on the pretension of the spokes. However, for simplicity, the pretension T_s in each spoke is assumed to be zero in the conventional finite element analysis and all numerical results of this paper are also obtained under this assumption except those presented in this subsection. Table 6 shows the influence of pretension T_s in each of the spokes on the lowest five natural frequencies of the bike beginning from T_s = 0 with increment $\Delta T_s = 100$ N. From the table one sees that increasing the pretension T_s will reduce the lowest five natural frequencies of the bike as has been shown in the previous subsection 2.4. Since a strong wheel relies on enough pretension T_s in each spoke and too high value of T_s will lead to buckling of the rim, determination of the appropriate pretension T_s in each spoke should be an optimum problem.

TABLE 6
INFLUENCE OF PRETENSION T_s IN EACH OF THE SPOKES ON THE LOWEST FIVE NATURAL FREQUENCIES OF THE BIKE

Pretension in each spoke, T_s (N)	Natural frequencies, ω_v (rad/sec)				
	ω_1	ω_2	ω_3	ω_4	ω_5
0 (cf. Table 4)	168.05399	207.60573	274.94635	311.38074	587.16357
100	166.28904	207.23125	274.11550	309.22295	587.07923
200	164.48525	206.83240	273.22357	307.11718	586.99563
300	162.64151	206.40621	272.26276	305.07272	586.91278
400	160.75661	205.94937	271.22524	303.09923	586.83066

5.4 Influence of rider mass (riding gesture) on the free vibration characteristics

In the previous subsections, the effect of rider mass is neglected and it will be studied in this subsection. It is well known that the mass of a rider is shared by the saddle and handlebar depending on the gesture of the rider. In this subsection, it is assumed that the total mass of the rider is 75 kg and it is shared by saddle and handlebar in three riding gestures: (i) $m_1 = 25$ kg and $m_{18} = 50$ kg; (ii) $m_1 = 18.75$ kg and $m_{18} = 56.25$ kg; (iii) $m_1 = 12.5$ kg and $m_{18} = 62.5$ kg. Where the subscripts of m, 1 and 18, refer to nodes 1 and 18 for the handlebar and saddle, respectively, as one may see from Fig. 5. It is noted that, for the last three riding gestures, the handlebar shares 1/3, 1/4 and 1/6 of the total rider mass, respectively, and the remaining 2/3, 3/4 and 5/6 of the total rider mass are shared by the saddle, respectively. For convenience, the above-mentioned three cases are called cases 1, 2 and 3 in Table 7, respectively, and the situation of no rider is called case 0. From Table 7 one sees that, in either riding gesture, the rider mass significantly affects the lowest five natural frequencies of the bike. To save the space, only the lowest five mode shapes of the bike for case 1 are shown in Fig. 8. Comparing with the lowest five mode shapes of the bike for case 0 shown in Fig. 7($a_1 - a_5$), one sees that the rider mass also significantly affects the lowest five mode shapes of the bike. From the foregoing analyses one sees that the influence of rider mass (and riding gesture) on the free vibration characteristics of a bike is a complicated problem and use of the information presented in the existing literature with rider mass neglected should be careful.

TABLE 7
INFLUENCE OF RIDER MASS (75 kg) ON THE LOWEST FIVE NATURAL FREQUENCIES OF THE BIKE

Case	Conditions	Natural frequencies, ω_v (rad/sec)				
		ω_1	ω_2	ω_3	ω_4	ω_5
0	No rider (cf. Table 4)	168.05399	207.60573	274.94635	311.38074	587.16357
1	$m_1 = 25$ kg , $m_{18} = 50$ kg	46.94273	72.29379	142.25082	182.86937	300.60258
2	$m_1 = 18.75$ kg , $m_{18} = 56.25$ kg	45.86708	73.52113	151.45699	193.60493	300.66467
3	$m_1 = 12.5$ kg , $m_{18} = 62.5$ kg	44.76827	74.62326	164.76774	215.10436	300.89367

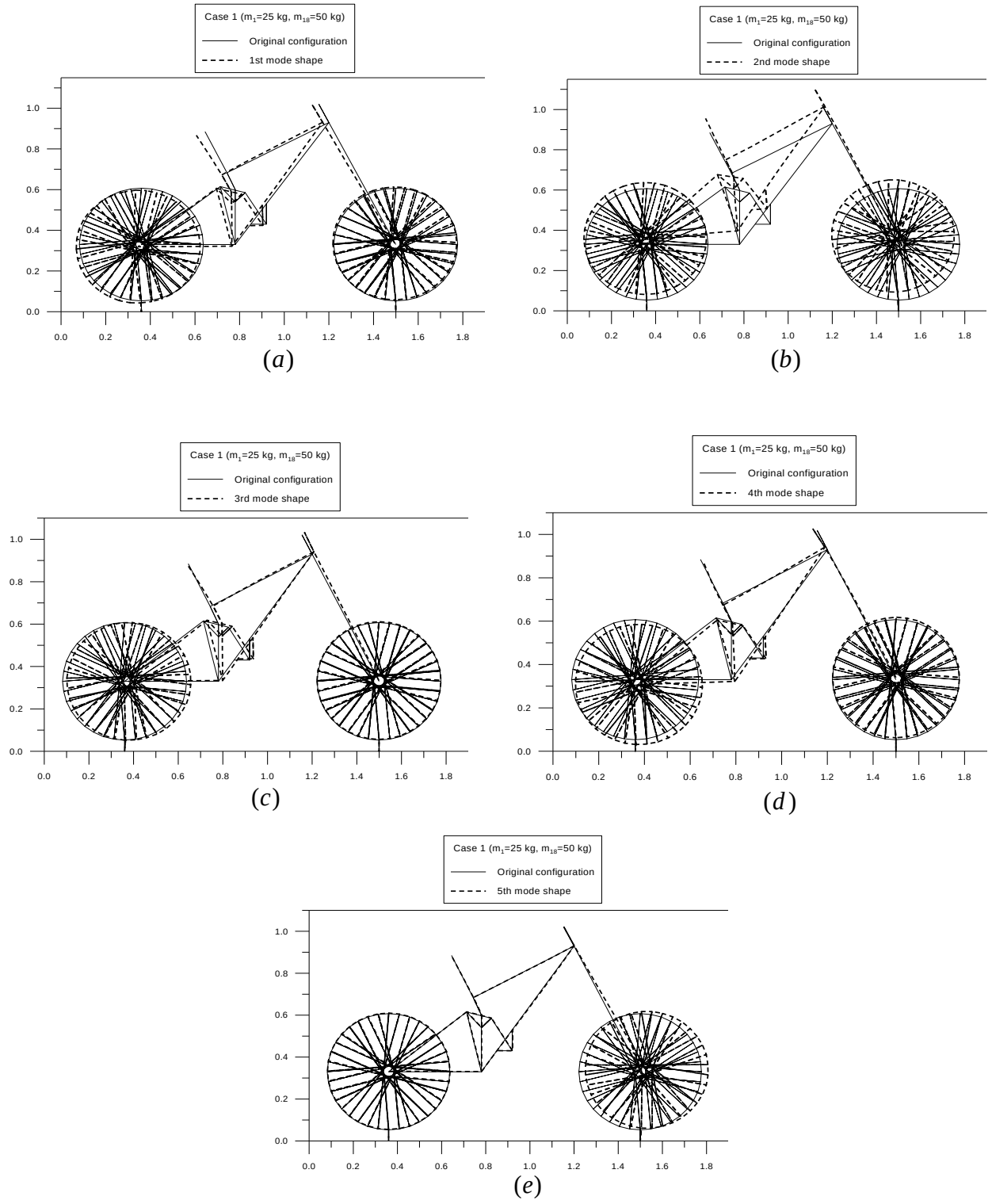

FIG. 8 INFLUENCE OF RIDER MASS (CASE 1) ON THE LOWEST FIVE MODE SHAPES OF THE BIKE

5.5 Influence of rider gesture on node displacements and internal forces of members

In the last subsection, it has been shown that different gesture of the rider will lead to different distribution of his mass on the handlebar and saddle. Of course, the gravitational forces on the bike induced by the rider are also dependent on the rider

gesture. For convenience, in this subsection, the rider gestures are assumed to be the same as those shown in Table 7, i.e.: (i) $F_1 = -25 \times 9.8 = -245$ N and $F_{18} = -50 \times 9.8 = -490$ N; (ii) $F_1 = -18.75 \times 9.8 = -183.75$ N and $F_{18} = -56.25 \times 9.8 = -551.25$ N; (iii) $F_1 = -12.5 \times 9.8 = -122.5$ N and $F_{18} = -62.5 \times 9.8 = -612.5$ N. Where the negative sign (-) indicates that the force F_1 (or F_{18}) is downward. The displacements of nodes 2, 11, 23, 34 and 35 (cf. Fig. 5) for the above-mentioned three cases are shown in Table 8(a) and the internal forces (and bending moments) of the five beam elements, 3, 9, 13, 37 and 40 are shown in Table 8(b). It is noted that the node displacements ($\bar{u}_x$ and $\bar{u}_y$) are with respect to the global $\bar{x}\bar{y}$ coordinate system with positive $\bar{u}_x$ agreeing with positive $\bar{x}$-axis and positive $\bar{u}_y$ agreeing with positive $\bar{y}$-axis (cf. Fig. 5). However, in the structural design, one requires the internal forces (and bending moments), F_x, F_y and M_z, at the two ends (with their node numberings ① and ②) of each beam element to be with respect to the local *xy* coordinate system (instead of the global $\bar{x}\bar{y}$ system) as shown in Table 8(b).

Based on Figs. 4 and 5, and case 1 of Table 8(b), one may obtain the free-body diagrams of beam element Nos. 3, 9, 13, 37 and 40 in the local xy coordinate systems as shown in Figs. 9(a)-(e), respectively. From Fig. 9(a) one sees that beam element No. 3 is subjected a "compressive" force with magnitude $F_x = 311.9$ N and from Fig. 9(d) one sees that beam element No. 37 is subjected a "tensile" force with magnitude $F_x = 436.01$ N. It is believed that the "tensile" force in chain stays (436.01 N) as shown in Fig. 9(d) being much greater than the "compressive" force in the front fork (311.9 N) as shown in Fig. 9(a) should be in agreement with the actual situations. Furthermore, the conditions of equilibrium, $\sum F_x = 0$, $\sum F_y = 0$ and $\sum M_z = 0$, are satisfied for each of the free-body diagrams shown in Figs. 9(a)-(e). In which, the length ℓ_i for the *i*-th beam element is determined by $\ell_i = \sqrt{(\bar{x}_{2,i} - \bar{x}_{1,i})^2 + (\bar{y}_{2,i} - \bar{y}_{1,i})^2}$ (*i* = 3, 9, 13, 37 or 40), with $(\bar{x}_{1,i}, \bar{y}_{1,i})$ and $(\bar{x}_{2,i}, \bar{y}_{2,i})$ representing the global coordinates of its node ① and node ② as shown in Fig. 2, respectively. It is noted that, in

TABLE 8 (*a*)
INFLUENCE OF RIDER'S GESTURE ON THE NODE DISPLACEMENTS

Cases	Displacements (m)	Numberings of nodes				
		2	11	23	34	35
1 $F_1 = -245$ N $F_{18} = -490$ N	$\bar{u}_x$	-0.2854E-03	-0.2470E-03	-.3349E-03	-.3380E-03	.3180E-03
	$\bar{u}_y$	-0.1626E-02	-0.1683E-02	-.1600E-02	-.9467E-03	-.6238E-03
2 $F_1 = -183.75$ N $F_{18} = -551.25$ N	$\bar{u}_x$	-.3909E-03	-.2914E-03	-.3031E-03	-.3064E-03	.2865E-03
	$\bar{u}_y$	-.1539E-02	-.1708E-02	-.1610E-02	-.1005E-02	-.5656E-03
3 $F_1 = -112.5$ N $F_{18} = -612.5$ N	$\bar{u}_x$	-.4964E-03	-.3358E-03	-.2713E-03	-.2749E-03	.2550E-03
	$\bar{u}_y$	-.1452E-02	-.1734E-02	-.1619E-02	-.1063E-02	-.5073E-03

Figs. 9(a)-(e), the counterclockwise (CCW) moments ($M_{z1,i}$ or $M_{z2,i}$) are positive because they are the bending moments about the positive z (or $\bar{z}$)-axis. Similar to Figs. 9(a)-(e), one may obtain the free-body diagrams of the beam element Nos. 3, 9, 13, 37 and 40 for the other cases of Table 8(b).

The configurations of the bike after deformations for the above-mentioned three cases (cf. Table 8) are shown in Figs. 10(a)-(c), respectively. In each case, all deformations (or displacements) of the nodes induced by the external forces F_1 and F_{18} are normalized by the maximum one in that case and then multiplied by a factor 0.05 to obtain the appropriate dimensions of the deformed bike for plotting. Because the external loads, F_1 and F_{18}, are downward and $F_1 < F_{18}$, all the vertical node displacements ($\bar{u}_y$) as shown in table 8 are in negative (-) $\bar{y}$-direction and all the horizontal node displacements ($\bar{u}_x$) as shown in same table are in negative (-) $\bar{x}$-direction (except those for node 35). It is the last reason, the deformations of the entire bike for the three cases have the same trend of tilting leftward, so that the deformed configurations of the bike for the three cases shown in Figs. 10(a)-(c) look similar. However, because the vertical force on the handlebar (F_1) is maximum in case 1 and minimum in case 3, so is the vertical deformation of node 2 near the handlebar (cf. Fig. 5) as one may see from Figs. 10 (a)-(c).

TABLE 8 (*b*)
INFLUENCE OF RIDER'S GESTURE ON THE INTERNAL MEMBER FORCES AND MOMENTS

Cases	Nodes	Forces (N) or moments (Nm)	Numberings of beam elements (Numbering of 1st node → Numbering of 2nd node)				
			3 (3→4)	9 (8→9)	13 (12→13)	37 (23→31)	40 (33→34)
1 $F_1 = -245$ N $F_{18} = -490$ N	①	F_x	.31190E+03	.46246E+03	-.46448E+03	-.43601E+03	-.43601E+03
		F_y	-.32154E+02	.16723E+03	-.60647E+02	.13000E+01	.13000E+01
		M_z	-.17975E+02	.13434E+02	.48521E+01	*0	-.40949E+00
	②	F_x	-.31190E+03	-.46246E+03	.46448E+03	.43601E+03	.43601E+03
		F_y	.32154E+02	-.16723E+03	.60647E+02	-.13000E+01	-.13000E+01
		M_z	.14380E+02	.83103E+01	-.12255E+02	.13650E+00	.54599E+00
2 $F_1 = -183.75$ N $F_{18} = -551.25$ N	①	F_x	.28249E+03.	.46990E+03	-.50805E+03	-.48138E+03	-.48138E+03
		F_y	-.29705E+02	.17371E+03	-.73535E+02	.14543E+01	.14543E+01
		M_z	-.16606E+02	.12482E+02	.21355E+01	0	-.45809E+00
	②	F_x	-.28249E+03	-.46990E+03	.50805E+03	.48138E+03	.48138E+03
		F_y	.29705E+02	-.17371E+03	.73535E+02	-.14543E+01	-.14543E+01
		M_z	.13285E+02	.10104E+02	-.11112E+02	.15270E+00	.61079E+00
3	①	F_x	.25308E+03	.47734E+03	-.55162E+03	-.52676E+03	-.52676E+03

$F_1 = -112.5$ N $F_{18} = -612.5$ N		F_y	-.27256E+02	.18019E+03	-.86424E+02	.16086E+01	.16086E+01
		M_z	-.15237E+02	.11531E+02	-.58119E+00	0	-.50669E+00
	②	F_x	-.25308E+03	-.47734E+03	.55162E+03	.52676E+03	.52676E+03
		F_y	.27256E+02	-.18019E+03	.86424E+02	-.16086E+01	-.16086E+01
		M_z	.12189E+02	.11898E+02	-.99682E+01	.16890E+00	.67559E+00

* Pivot at node 23.

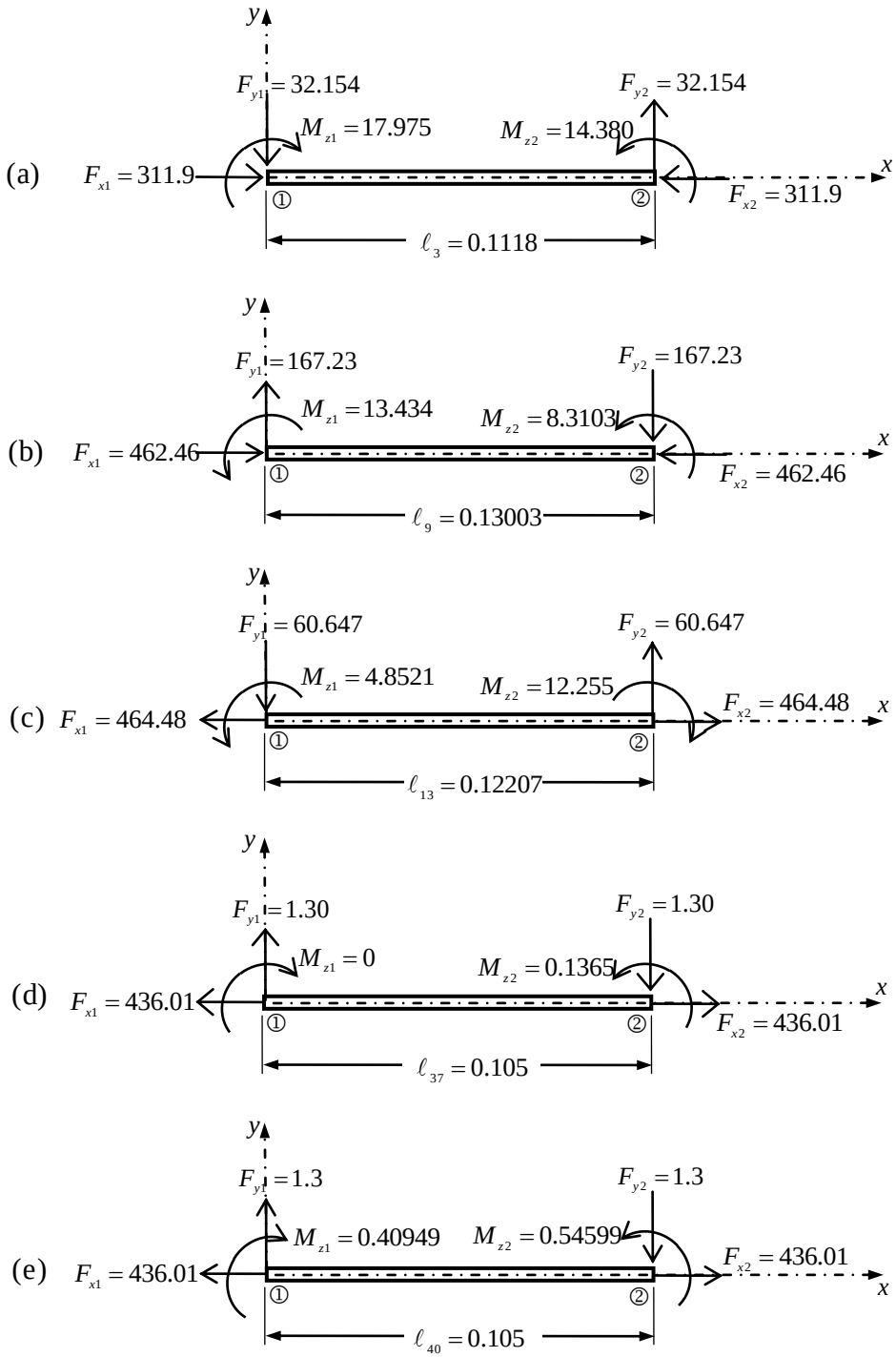

FIG. 9 FREE-BODY DIAGRAMS FOR NOS. (*a*) 3, (*b*) 9, (*c*) 13, (*d*) 37 AND (*e*) 40 BEAM ELEMENTS BASED ON FIGS. 4 AND 5, AND CASE 1 OF TABLE 8(*b*). ALL BEAM ELEMENTS ARE C-C EXCEPT NO. 37 BEAM ELEMENT IN (*d*) BEING P-C.

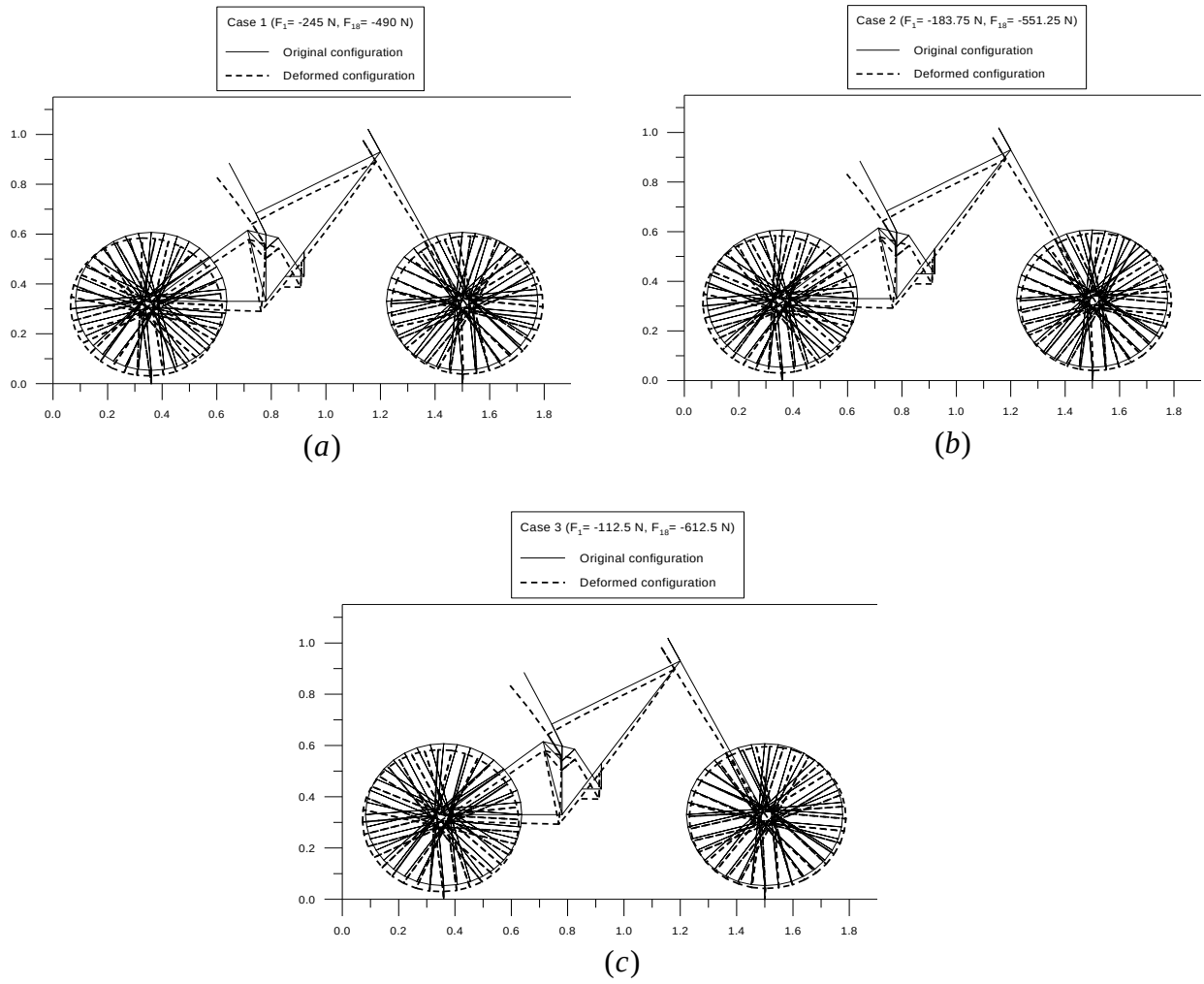

FIG. 10 THE DEFORMED CONFIGURATIONS OF THE ENTIRE BIKE SUBJECTED GRAVITATIONAL FORCES OF THE RIDER: (*a*) CASE 1; (*b*) CASE 2; (*c*) CASE 3.

VI. CONCLUSION

Based on the foregoing numerical-analysis results, the following conclusions are drawn:

1. Because the ratio of the lumped masses of attachments (including the two tires) to total mass of the structural members (contributed to the stiffness of the entire bike) is high (near 50%), the dynamic analysis of a bike should be conducted with the effect of its lumped masses of attachments considered.

2. The "moment arm" for the tensile force in each spoke with respect to the hub center increases with the increase of radius r_h of the hub disk, so does the restoring moment induced by the spoke tension. Thus, the effective stiffness of the sub-structural system composed of the rim, spokes and hub (disks) increases with the increase of r_h and so do the lowest several natural frequencies of the entire bike.

3. Because the compressive force T_r in a rim induced by the pretension of all its spokes is much larger than the pretension T_s in each spoke, in spite of the fact that the pretension T_s can raise the stiffness of each spoke and the compressive force T_r can reduce the stiffness of the rim, the overall effect of increasing the pretension T_s will reduce the overall stiffness of the sub-structural system composed of hub (disk), spokes and rim, thus, the lowest several natural

frequencies of the bike will decrease with the increase of pretension T_s. Since a strong wheel relies on enough pretension T_s in each spoke and too high value of T_s will lead to buckling of the rim, determination of the appropriate pretension T_s in each spoke should be an optimum problem.

4. The free vibration characteristic of a bike is significantly affected by the mass of its rider. Thus, for a bike to accommodate various riders, some of its pertinent parameters (e.g., the axial stiffness of the "spring-damper units" for rear and front suspension systems) should be adjustable. In addition, most of information obtained from the bike without a rider in the existing literature, its applicability in practice seems to need further studies.

5. For a bike subjected to the gravitational forces of a rider, its node displacements and internal forces (and bending moments) of the structural members are significantly affected by the riding gesture of the rider. Based on the theory presented and the computer program developed for this paper one may easily obtain the last information, this should be benefit for designing a save and comfortable bike.

REFERENCES

[1] Champoux, Y., Richard, S. and Drouet, J.M. (2007) Bicycle Structural Dynamics. Sound and Vibration, 16-22, http://www.SandV.com.

[2] Levy, M. and Smith, G.A. (2005) Effectiveness of vibration damping with bicycle suspension systems. Sports Engineering, 8, 99 - 106.

[3] Good, C. and McPhee, J. (1999) Dynamics of mountain bicycles with rear suspensions: modeling and simulation. Sports Engineering, 2, 129 -143.

[4] Wu, C.C. (2013) Static and dynamic analyses of mountain bikes and their riders. Ph.D. thesis, Department of Mechanical Engineering, University of Glasgow, UK.

[5] Padilla, M. and Brennan, J. (1996) Bicycle rear suspension study. Human Power Lab, Cornell University, USA.

[6] Good, C. and McPhee, J. (2000) Dynamics of mountain bicycles with rear suspensions: design optimization. Sports Engineering, 3, 49 -55.

[7] Karchin, A. and Hull, M.L. (2002) Experimental optimization of pivot point height for swing-arm type rear suspensions in off-road bicycles. Journal of Biomechanical Engineering, 124, 101-106.

[8] Wang, E.L. and Hull, M.L. (1997) Minimization of pedalling induced energy losses in off-road bicycle rear suspension systems. Vehicle System Dynamics, 28(4), 291-306.

[9] Przemieniecki, J.S. (1968) Theory of Matrix Structural Analysis. McGraw-Hill, Inc., New York.

[10] Beaufait, F.W., JR Rowan, W.H., Hoadley, P.G. and Hackett, R.M. (1970) Computer Methods of Structural Analysis, Prentice-Hall, Inc., London.

[11] Wu, J.S. and Chiang, L.K. (2004) Free vibration of a circularly curved Timoshenko beam normal to its initial plane using finite curved beam elements. Computers & Structures, 82, 2525-2540.

[12] Clough, R.W. and Penzien, J. (1975) Dynamics of Structures. McGraw-Hill, Inc., New York.

[13] Bathe, K.J. (1982) Finite Element Procedures in Engineering Analysis. Prentice-Hall, Inc., Englewood Cliffs, New Jersey.

Appendix A

Stiffness and mass matrices of the P-P, P-C and C-C beam elements

The stiffness matrix $[k]_{PP}$ and mass matrix $[m]_{PP}$ for the P-P beam element are given by [9]

$$[k]_{PP} = \left[\begin{array}{cc:cc} EA/\ell & 0 & -EA/\ell & 0 \\ 0 & 0 & 0 & 0 \\ \hdashline -EA/\ell & 0 & EA/\ell & 0 \\ 0 & 0 & 0 & 0 \end{array}\right] \qquad \text{(A.1)}$$

$$[m]_{PP}=\left[\begin{array}{cc:cc} \rho A\ell/3 & 0 & \rho A\ell/6 & 0 \\ 0 & 0 & 0 & 0 \\ \hdashline \rho A\ell/6 & 0 & \rho A\ell/3 & 0 \\ 0 & 0 & 0 & 0 \end{array}\right] \tag{A.2}$$

The stiffness matrix $[k]_{PC}$ and mass matrix $[m]_{PC}$ for the P-C beam element are given by [10]

$$[k]_{PC}=\left[\begin{array}{cc:ccc} EA/\ell & 0 & -EA/\ell & 0 & 0 \\ 0 & 3EI/\ell^3 & 0 & -3EI/\ell^3 & 3EI/\ell^2 \\ \hdashline -EA/\ell & 0 & EA/\ell & 0 & 0 \\ 0 & -3EI/\ell^3 & 0 & 3EI/\ell^3 & -3EI/\ell^2 \\ 0 & 3EI/\ell^2 & 0 & -3EI/\ell^2 & 3EI/\ell \end{array}\right] \tag{A.3}$$

$$[m]_{PC}=\frac{\rho A\ell}{420}\left[\begin{array}{cc:ccc} 140 & 0 & 70 & 0 & 0 \\ 0 & 35 & 0 & -17.5 & 3.5\ell \\ \hdashline 70 & 0 & 140 & 0 & 0 \\ 0 & -17.5 & 0 & 113.75 & -12.25\ell \\ 0 & 3.5\ell & 0 & -12.25\ell & 1.75\ell^2 \end{array}\right] \tag{A.4}$$

The stiffness matrix $[k]_{CC}$ and mass matrix $[m]_{CC}$ for the C-C beam element are given by [9]

$$[k]_{CC}=\left[\begin{array}{ccc:ccc} EA/\ell & 0 & 0 & -EA/\ell & 0 & 0 \\ 0 & 12EI/\ell^3 & 6EI/\ell^2 & 0 & -12EI/\ell^3 & 6EI/\ell^2 \\ 0 & 6EI/\ell^2 & 4EI/\ell & 0 & -6EI/\ell^2 & 2EI/\ell \\ \hdashline -EA/\ell & 0 & 0 & EA/\ell & 0 & 0 \\ 0 & -12EI/\ell^3 & -6EI/\ell^2 & 0 & 12EI/\ell^3 & -6EI/\ell^2 \\ 0 & 6EI/\ell^2 & 2EI/\ell & 0 & -6EI/\ell^2 & 4EI/\ell \end{array}\right] \tag{A.5}$$

$$[m]_{CC}=\frac{\rho A\ell}{420}\left[\begin{array}{ccc:ccc} 140 & 0 & 0 & 70 & 0 & 0 \\ 0 & 156 & 22\ell & 0 & 54 & -13\ell \\ 0 & 22\ell & 4\ell^2 & 0 & 13\ell & -3\ell^2 \\ \hdashline 70 & 0 & 0 & 140 & 0 & 0 \\ 0 & 54 & 13\ell & 0 & 156 & -22\ell \\ 0 & -13\ell & -3\ell^2 & 0 & -22\ell & 4\ell^2 \end{array}\right] \tag{A.6}$$